Wong VC, Chen H, Ko JM, Chan KW, Chan YP, Law S et al.. Tumor suppressor Dual-specificity Phosphatase 6 (DUSP6) impairs cell invasion and epithelial-mesenchymal transition (EMT)-as...

ARTICLE *in* INTERNATIONAL JOURNAL OF CANCER · JANUARY 2012

Impact Factor: 5.09 · DOI: 10.1002/ijc.25970 · Source: PubMed

UICC
global cancer control

IJC
International Journal of Cancer

Tumor suppressor dual-specificity phosphatase 6 (DUSP6) impairs cell invasion and epithelial-mesenchymal transition (EMT)-associated phenotype

Victor Chun Lam Wong[1], Han Chen[2], Josephine Mun Yee Ko[1], Kwok Wah Chan[3], Yuen Piu Chan[3], Simon Law[4], Daniel Chua[1], Dora Lai-Wan Kwong[1], Hong Lok Lung[1], Gopesh Srivastava[3], Johnny Cheuk On Tang[5], Sai Wah Tsao[6], Eugene R. Zabarovsky[7,8], Eric J. Stanbridge[9] and Maria Li Lung[1]

[1] Department of Clinical Oncology and Center for Cancer Research, University of Hong Kong, Hong Kong (SAR), People's Republic of China
[2] Division of Life Science, Hong Kong University of Science and Technology, Hong Kong (SAR), People's Republic of China
[3] Department of Pathology, University of Hong Kong, Hong Kong (SAR), People's Republic of China
[4] Department of Surgery, University of Hong Kong, Hong Kong (SAR), People's Republic of China
[5] Department of Applied Biology and Chemical Technology, Hong Kong Polytechnic University, Hong Kong SAR, People's Republic of China
[6] Department of Anatomy, University of Hong Kong, Hong Kong (SAR), People's Republic of China
[7] Department of Microbiology, Tumor and Cell Biology, Karolinska Institute, Stockholm, Sweden
[8] Laboratory of Structural and Functional Genomics, Engelhardt Institute of Molecular Biology, Russian Academy of Sciences, Moscow, 119991, Russia
[9] Department of Microbiology and Molecular Genetics, University of California, Irvine, CA

Suppressive effects of DUSP6 in tumorigenesis and EMT-associated properties were observed. Dual-specificity phosphatase (DUSP6) is a MAP kinase phosphatase (MKP) negatively regulating the activity of ERK, one of the major molecular switches in the MAPK signaling cascade propagating the signaling responses during malignancies. The impact of DUSP6 in EMT and its contribution to tumor dissemination has not yet been characterized. Due to differences in tumor microenvironments affecting cell signaling during cancer progression, DUSP6 may play varying roles in tumor development. We sought to examine the potential role of DUSP6-mediated tumorigenesis and EMT-associated properties in two aerodigestive tract cancers, namely, esophageal squamous cell carcinoma (ESCC) and nasopharyngeal carcinoma (NPC). Significant loss of DUSP6 was observed in 100% of 11 ESCC cell lines and 71% of seven NPC cell lines. DUSP6 expression was down-regulated in 40% of 30 ESCC tumor tissues and 75% of 20 NPC tumor tissues compared to their respective normal counterparts. Suppressive effects of DUSP6 in tumor formation and cancer cell mobility are seen in *in vivo* tumorigenicity assay and *in vitro* colony formation, three-dimensional Matrigel culture, cell migration and invasion chamber tests. Notably, overexpression of DUSP6 impairs EMT-associated properties. Furthermore, tissue microarray analysis reveals a clinical association of DUSP6 expression with better patient survival. Taken together, our study provides a novel insight into understanding the functional impact of DUSP6 in tumorigenesis and metastasis of ESCC and NPC.

Key words: dual-specificity phosphatase 6 (DUSP6), tumor suppression
Additional Supporting Information may be found in the online version of this article.
V.C.L.W. and H.C. contributed equally to this work.
Grant sponsors: The University Grants Council Area of Excellence grant and the University of Hong Kong Seed Funding (MLL) Programme for Basic Research, the Swedish Cancer Society, the Swedish Research Council, the Swedish Institute, Karolinska Institute (ERZ)
DOI: 10.1002/ijc.25970
History: Received 13 Aug 2010; Accepted 30 Dec 2010; Online 3 Feb 2011
Correspondence to: Maria Li Lung, Room L2-23, 2/F, Laboratory Block, Department of Clinical Oncology, The University of Hong Kong, 21 Sassoon Road, Pokfulam, Hong Kong, HKSAR, People's Republic of China, Fax: 852-2819-5872, E-mail: mlilung@hku.hk

Intracellular signaling by MAP kinases tightly regulates cellular responses from various physiological stimuli. The equilibrium between activated MAPKs and the phosphatases plays a key physiopathological role during cancer transformation. ERK1/2 is one of the major molecular switches in this MAPK signaling cascade.[1] Oncogenic mutations often occur in the ERK/MAPK signaling pathways, including mutations of receptor tyrosine kinases, Ras GTPase and serine/threonine MAPK kinase kinase.[2] The Ras-ERK pathway is involved in greater than 30% of human breast cancers.[3] Crucial negative regulators of the ERK/MAPK signaling cascade include the MAP kinase phosphatases (MKPs), which belong to the dual-specificity phosphatase (DUSP) family. They control the activity of MAPK signaling transduction by dephosphorylating both threonine and tyrosine residues on their targets.[4] Accumulating evidence over the years has

implicated the important role of the ERK signaling pathway in tumorigenesis.

DUSPs act differently and may even play opposing roles in various cancers depending on types and progression. Specifically, DUSP6 acts as a negative feedback regulator for ERK1/2, by dephosphorylating the threonine and tyrosine residues.[1,5] It is functionally involved in suppressing tumor progression in pancreatic, ovarian and lung cancers.[6–9] Its down-regulated expression was observed in primary ovarian cancer. In lung cancer, DUSP6 is progressively lost, as tumor grading increases.[9] The down-regulation of *DUSP6* is attributed to epigenetic silencing and 12q21 allelic loss.[6,10] Earlier studies indicate that DUSP6 suppresses cell proliferation in lung and ovarian cancers[8,9] and promotes apoptosis in lung and pancreatic cancers.[6,8] Loss of DUSP6 contributes to resistance to cisplatin-induced apoptosis in ovarian cancer.[8] However, several lines of evidence also suggest an opposite role for DUSP6, which is counterintuitive to the proposed tumor suppressive function just mentioned. First, DUSP6 shows prosurvival ability in HeLa cells.[11] Second, DUSP6 is highly expressed in tamoxifen-resistant metastatic lesions. Overexpression of DUSP6 shows a higher tumor growth rate in tamoxifen-treated animals compared to controls.[12] Third, depletion of DUSP6 promotes apoptosis in breast cancer.[13] Fourth, methylation of *DUSP6* is an infrequent event in endometrial cancer.[14] The detailed explanation for the discrepancy is as yet unknown, but may be attributed to individual cancer differences.

Esophageal squamous cell carcinoma (ESCC) and nasopharyngeal carcinoma (NPC) are aerodigestive tract cancers with especially high incidence in China.[15,16] *DUSP6* maps to chromosome 12q, a commonly deleted region observed in both cancers.[17,18] DUSP6 is involved in the pathogenesis of NPC.[19] It is also a downstream candidate gene associated with *deleted in esophageal cancer 1* (*DEC1*), a frequently down-regulated gene in ESCC suppressing anchorage-independent growth *in vitro* and tumor formation *in vivo*.[20,21] ERK1/2, which promotes cancer cell proliferation in ESCC[22] and NPC,[23] has recently been shown to induce EMT.[24] This suggests its specific negative regulator, DUSP6, may also contribute to EMT. Little is known about the pathophysiological effects of DUSP6 in NPC and ESCC tumorigenesis. To our knowledge, the potential impact of DUSP6 in EMT, a crucial event conferring onto cancer cells a migration ability and propensity to disseminate, has not yet been reported. Therefore, we aim to evaluate the role of DUSP6 in ESCC and NPC tumorigenesis and EMT-associated properties. The expression of DUSP6 in cell lines and tissue biopsies and the mechanism involved in its silencing in these tumors was investigated. The functional impact of DUSP6 in tumorigenesis and EMT-associated properties was examined by *in vitro* and *in vivo* assays. Additionally, the clinical relevance of DUSP6 in cancer development was explored.

Material and Methods

Cell lines, culture conditions and clinical specimens

Sixteen ESCC cell lines (SLMT-1, HKESC-2, TTn6, 81T, KYSE30, KYSE70, KYSE140, KYSE150, KYSE180, KYSE270, KYSE410, KYSE450, KYSE510, KYSE520, EC1 and EC18) were cultured in Dulbecco's modified eagle medium (DMEM) supplemented with 5% fetal bovine serum (FBS) (Life Technologies, Carlsbad, CA) and an immortalized normal esophageal epithelial cell line (NE1) was cultured in keratinocyte-serum free medium (KSFM) (Invitrogen, Carlsbad, CA), as previously described.[25] Ten Japanese cell lines, KYSE30/70/140/150/180/270/410/450/510/520 are commercially available from the DSMZ (Braunschweig, Germany).[26] The immortalized nasopharyngeal epithelial cell line, NP460, was cultured in 50% defined KSFM and 50% epilife medium (Invitrogen, Carlsbad, CA), as described.[27] The NPC cell lines, HONE-1, CNE1, CNE2, HNE1, SUNE1, HK1, C-666 and the tetracycline transactivator (tTA)-producing cell line HONE1-2, were cultured as previously described.[28,29] ESCC patient tissue specimens between 2001 and 2003 and NPC biopsies in 2006 were collected from Queen Mary Hospital, as previously described.[25,29]

Bisulfite sequencing, demethylation treatment and microsatellite analysis

The primer pairs for *DUSP6* bisulfite sequencing were designed by MethPrimer primer design program (www.urogene.org/methprimer). Forward: 5′-GGGGGTGTTAGT AGGTATGTT-3′; Reverse: 5′-TACAAAACCAA CAAATAA CTTTAAAAAA-3′. In brief, 1 μg genomic DNA was bisulfite-modified using the CpGenome^{TM} DNA Modification Kit (Chemicon International, Inc., Temecula, CA) and modified DNA was subjected to PCR. The amplified bisulfite-treated region was then subcloned into the pMD19-T vector (TAKARA BIO INC, Shiga, Japan). Ten clones from each sample were sequenced. For demethylation drug treatment, the ESCC cell lines were first cultured in 100 mm plates until 40% confluent and subsequently treated with 2 μM 5-aza-2'-deoxycytidine (Sigma, St Louis, MO) for 5 days, as previously described.[25] Microsatellite analysis was performed using fluorescent PCR-based analysis on an Applied Biosystems Prism 3100 Genetic Analyzer (Applied Biosystem, Foster City, CA), as previously described.[25] Sequences for five microsatellite markers (D12S1719, D12S82, D12S1567, D12S1064 and D12S351), which map from 87.16 to 91.90 Mb on the 12q21 region, are available from the NCBI genomic database (http://www.ncbi.nlm.nih.gov/). Each allele of tissue specimens was scored by comparing the ratio of the signal intensities between the tumor (T) and its corresponding normal (N) tissue specimen in heterozygous alleles based on the formula T1:T2/N1:N2, where N1 and N2 stand for higher and lower peak heights, respectively, for the alleles present in the normal tissue, while T1 and T2 refer to their corresponding alleles present in the tumor specimen. When the value was

<0.67 or >1.5, the allele was scored as allelic loss. This lower stringency cut-off value was used as reported previously[25] and as detailed in the Applied Biosytems User's Manual.

Quantitative RT-PCR analysis

The total RNAs of cell lines and patient specimens were extracted using TRIzol reagent according to manufacturer's protocol (Invitrogen, Carlsbad, CA). Total RNAs were then converted to cDNA using M-MLV Reverse Transcriptase (USB, Cleveland, OH). The expression levels of *DUSP6* were then examined by quantitative RT-PCR using the StepOnePlus RealTime PCR system (Applied Biosystem, Foster City, CA). The *DUSP6* and *GAPDH* Taqman probes were purchased from Applied Biosystems (Foster City, CA).

Western blot analysis

Preparation of cell lysates, protein electrophoresis and transfer were as previously described.[25] Primary antibody incubation was performed with FG-07 antibody for DUSP6 (1:1000; Santa Cruz Biotechnology, Santa Cruz, CA), 36/E-Cadherin antibody for E-cadherin (1:1000; BD Biosciences, Labware, MA) and RV202 antibody for vimentin (1:1000; BD Biosciences, Labware, MA). Ab-1 antibody (1:10,000; Calbiochem, Darmstadt, Germany) for detecting alpha-tubulin was used as a loading control. L34F12 and D13.14.4E antibodies for ERK1/2 and Phospho-ERK1/2 (1:1000; Cell Signaling Technology, MA) were also used.

Stable transfection of *DUSP6* and colony formation assay

The *DUSP6* 1.1 kb cDNA fragment was subcloned from pOTB7-*DUSP6* (Catalog no. MGC-3789, ATCC, Manassas, VA) into pCR3.1 (Invitrogen, Grand Island, NY) at the BamHI/XhoI restriction site, and then subsequently cloned into pETE-Bsd using the NheI and XbaI sites.[28] To generate *DUSP6* stably expressing clones, SLMT-1 and HONE1-2 were transfected with pCR3.1-*DUSP6* and pETE-Bsd-*DUSP6*, respectively, as previously described.[25,29] SLMT-1 stable clones were cultured in 400 μg/ml G418 (Geneticin) (Invitrogen, Grand Island, NY). Construction of a pETE-Bsd–responsive vector and engineering of a HONE1 cell line, HONE1-2, which expresses the tetracycline transactivator tTA, was described by Protopopov et al.[28] Stable clones of HONE1-2 were maintained in culture medium containing 500 μg/ml G418 geneticin and 5 μg/mL blasticidin. Colony formation assay was performed using pCR3.1, as previously described.[25]

In vivo tumorigenicity assay

For each cell line, a total of six sites of three 6–8 week old female athymic Balb/c Nu/Nu mice were subcutaneously injected with 5×10^6 cells for SLMT-1 and 1×10^7 for HONE1-2. Tumor volume was measured weekly using calipers. To turn-off *DUSP6* expression in *DUSP6* stable clones, 200 μg/ml doxycycline was added to drinking water of mice starting 1 week before injection.

Fluorescence staining

Fluorescence staining of cells was performed as previously described.[21] For staining the cell spheroids in three-dimensional culture, cells were fixed in 2% formalin for 15 min at room temperature and then permeabilized with 1% Triton X-100 in PBS for 15 min. Actin staining was then performed with rhodamine phalloidin (Invitrogen, Carlsbad, CA), according to manufacturer's protocol. The nucleus was stained with 4,6-diamidino-2-phenylindole (DAPI).[21] Images were captured by inverted fluorescence microscopy (Nikon Instruments, Ontario, Canada).

Soft agar and Matrigel culture assays

Soft agar assay and Matrigel culture were performed as previously described.[21,25] For Matrigel BD (Biosciences Discovery Labware, MA) culture, 2000 cells were seeded on top of Matrigel. Images were captured using inverted fluorescence microscopy (Nikon Instruments, Ontario, Canada) and colonies were counted. At least 50 colonies were used for size measurement.

Wound healing, cell migration and invasion assays

Cell lines were cultured until confluent. Thereafter, the cell monolayer was then scratched with a pipette tip and incubated for 1 day. The relative wound areas were calculated: (migrated distance of *DUSP6* expressing clones/ migrated distance of vector-alone stable clones) × 100. Cell migration and invasion chamber assays were performed, as previously described.[21,25] The relative cell migration/invasion ability was calculated (the number of migrated cells in *DUSP6* stable clones/the number of migrated cells in vector-alone stable clones) × 100. DAPI was used to stain cells for quantification in cell migration and invasion chamber assays.

Tissue microarray (TMA) and immunohistochemical (IHC) staining

A TMA of ESCC was constructed as previously described.[30] It contained ESCC tumor tissues from 74 consecutive Chinese patients who underwent total esophagectomy for previously untreated ESCC in Queen Mary Hospital in Hong Kong from 1998 to 2005. Supplementary Table 1 shows the clinical information of these patients. IHC staining was performed as previously described,[30] with FG-07 antibody for DUSP6 (1:100; Santa Cruz Biotechnology, Santa Cruz, CA) as the primary antibody. As shown in Supplementary Fig. 1, the specificity of the FG-07 antibody in recognizing DUSP6 expression was confirmed by immunostaining after transient transfection of pCR3.1-*DUSP6* and pCR3.1 expression vector into an ESCC cell line, KYSE520. The stained sections were examined by a pathologist (KW Chan), who had no prior knowledge of the clinicopathological data of the patients. The intensity of staining was graded by an arbitrary scale that ranged from 0 to 3, representing negative ("0"), weak ("1"), moderate ("2") and strong ("3") staining, respectively.

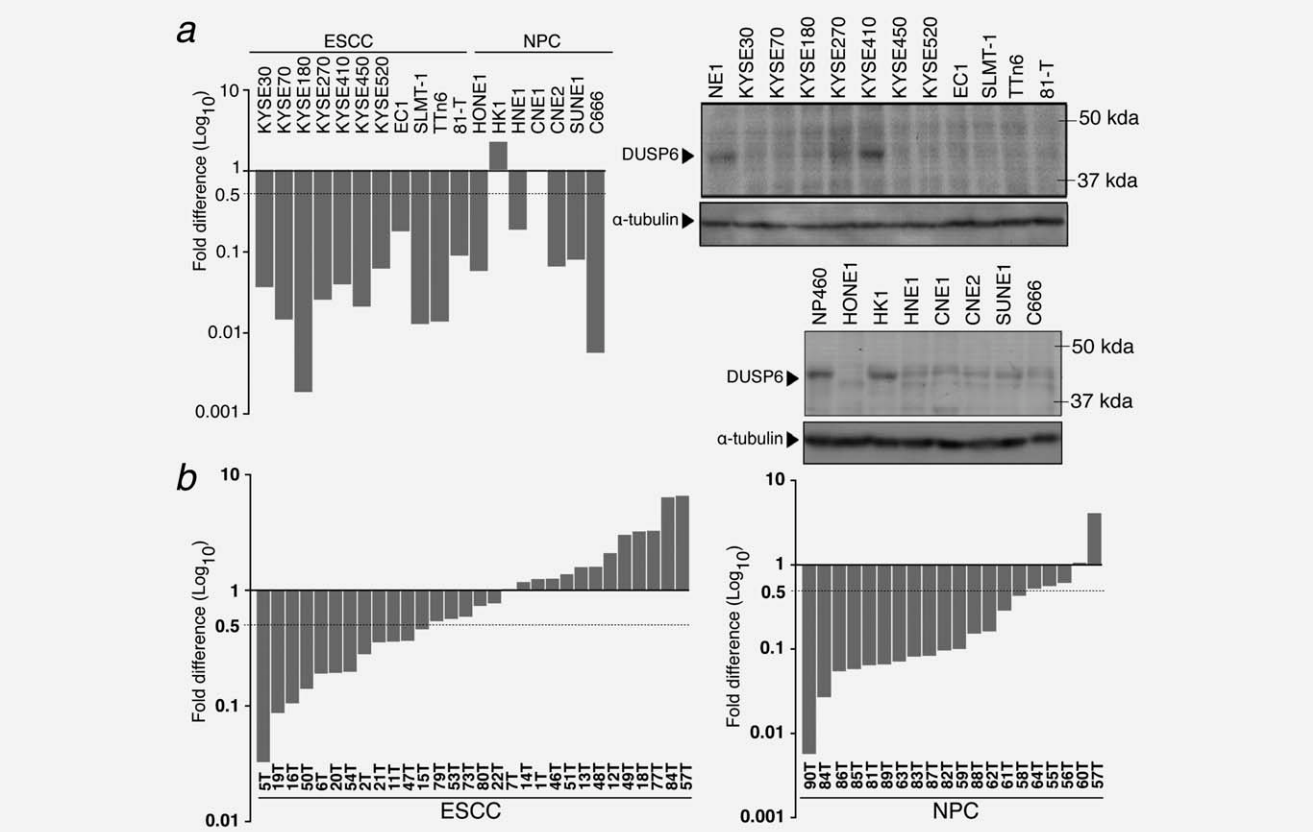

Figure 1. Expression analysis of DUSP6 in cell lines and tissues. (*a*) Left panel: By quantitative RT-PCR, 100% (11/11) of the ESCC cell line panel and 71% (5/7) of the NPC cell line panel show at least 2-fold down-regulation of *DUSP6* at the mRNA level compared to NE1 and NP460, respectively. NE1 is an immortalized normal esophageal epithelial cell line, while NP460 is an immortalized nasopharyngeal epithelial cell line; they serve as positive controls. Right panel: immunoblotting analysis of DUSP6. Loss of DUSP6 was also observed in immunoblot analysis of ESCC (upper) and NPC (lower) cell lines. (*b*) By quantitative RT-PCR of paired normal and tumor tissues from the same patients, 40% (12/30) of the ESCC biopsies and 75% (15/20) of the NPC biopsies show at least 2-fold down-regulation of *DUSP6* compared to their corresponding normal counterparts. Two-fold threshold of down-regulation is indicated by dashed line.

Staining values of 0 and 1 were classified as low expression, while 2 and 3 were classified as high expression.

Statistical analysis

Statistical comparison of the data in colony formation, migration and invasion assays, Matrigel culture and tumor volume between the vector-alone and *DUSP6* stable transfectants were performed with the Student's *t*-test. Associations between clinical pathological information of ESCC patients and expression of *DUSP6* were analyzed using SPSS. All p values of less than 0.05 were considered to be statistically significant. Correlation of DUSP6 expression and patient survival was analyzed by Kaplan–Meier statistical analysis.

Results

Frequently down-regulated expression of DUSP6 and epigenetic silencing in ESCC and NPC

We examined the expression of DUSP6 in ESCC and NPC cell lines by quantitative RT-PCR and Western blots and found 100% (11/11) of the ESCC and 71% (5/7) of the NPC cell line panels show down-regulation of DUSP6 at the mRNA and protein levels compared to an immortalized normal esophageal epithelial cell line, NE1, and an immortalized nasopharyngeal epithelial cell line, NP460, respectively (Fig. 1*a*). ERK1/2 is more active in ESCC and NPC cancer cell lines compared to the immortalized normal epithelial cell lines, suggesting loss of a negative feedback mechanism to induce DUSP6 to restrain ERK activity in cancer cell lines (Supplementary Fig. 2). For tumor tissues, 40% (12/30) of the ESCC biopsies and 75% (15/20) of the NPC biopsies show at least 2-fold down-regulation of *DUSP6* in the tumors as compared to their corresponding normal counterparts (Fig. 1*b*). These observations of frequent loss of DUSP6 in cell lines and tumors suggest its important role in tumorigenesis.

We evaluated the role of epigenetic silencing in the down-regulation of *DUSP6*. DUSP6 expression was restored in two ESCC (SLMT-1 and KYSE30) and two NPC cell lines (HONE1 and CNE2) after DNA demethylation treatment (Fig. 2*a*). PROSCAN (http://www-bimas.cit.nih.gov/molbio/proscan/) identified a putative promoter at location −1581 to 1331 relative to

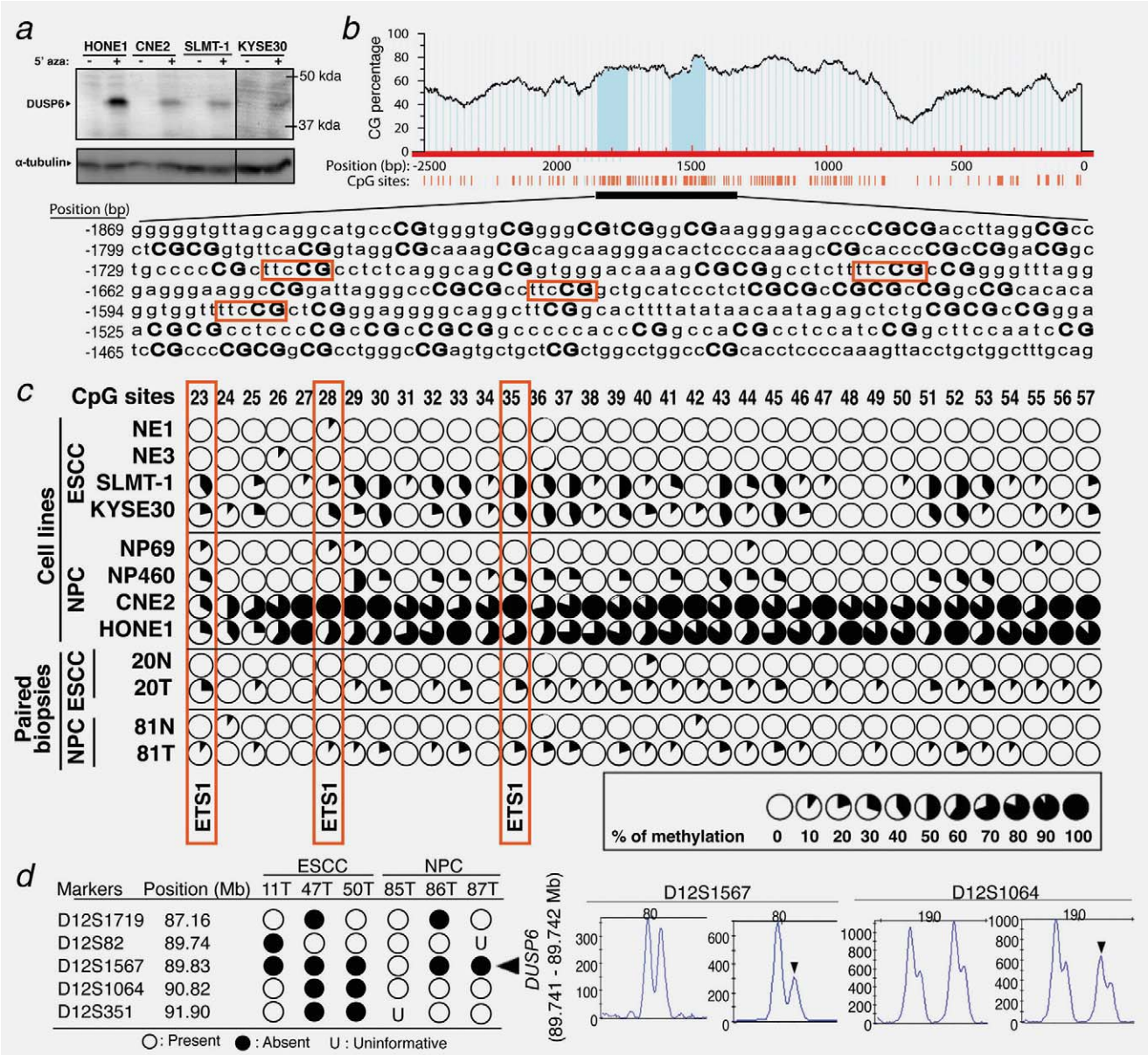

Figure 2. Epigenetic and genetic inactivation mechanisms of *DUSP6*. (*a*) Western blot analysis shows restoration of *DUSP6* expression in two ESCC (SLMT-1 and KYSE30) and two NPC (HONE1 and CNE2) cell lines after demethylation treatment by 5′-aza-2′-deoxycytidine. (*b*) Region of CpG sites in *DUSP6* analysis by bisulfite genomic sequencing. The Methprimer website identified the richest CpG sites located from −1869 to −1379 relative to the transcriptional start site of *DUSP6*. Fifty-seven CpG sites are included (bolded). E-26 transcription factors (ETS) are known downstream targets of ERK1/2 signaling (Ref. 31), regulating *DUSP6* expression (Ref. 32). The ETS1 transcription factor binding regions are shown (red boxed) (*c*) Methylation status of the CpG sites in cell lines and paired biopsies (25 CpG sites were shown). NE1 and NE3 are immortalized normal esophageal epithelial cell lines. NP460 and NP69 are immortalized nasopharyngeal epithelial cell lines. Methlyation of CpG sites in tumor cell lines and biopsies was higher than that observed in the corresponding immortalized cell lines and normal tissue counterparts, respectively. The ETS1 transcription factor binding regions are shown (red boxed); they show higher methylation in tumor cell lines and tumor biopsies. (*d*) Microsatellite analysis of chromosome 12q21 region in ESCC and NPC paired biopsies. Left panel: Allelic loss was observed in tumor biopsies, as compared to their normal counterparts. The highest frequency of loss was observed for the D9S1567 marker, which maps in the *DUSP6* region. Right panel: Representative microsatellite typing of one paired normal (N) and tumor (T) tissue, 47N/T, for the D12S1567 and D12S1064 markers. The scales on the top and left sides of each figure represent the size (bp) and the signal intensity, respectively. (▼) indicates allelic loss observable in tumor specimens. [Color figure can be viewed in the online issue, which is available at wileyonlinelibrary.com.]

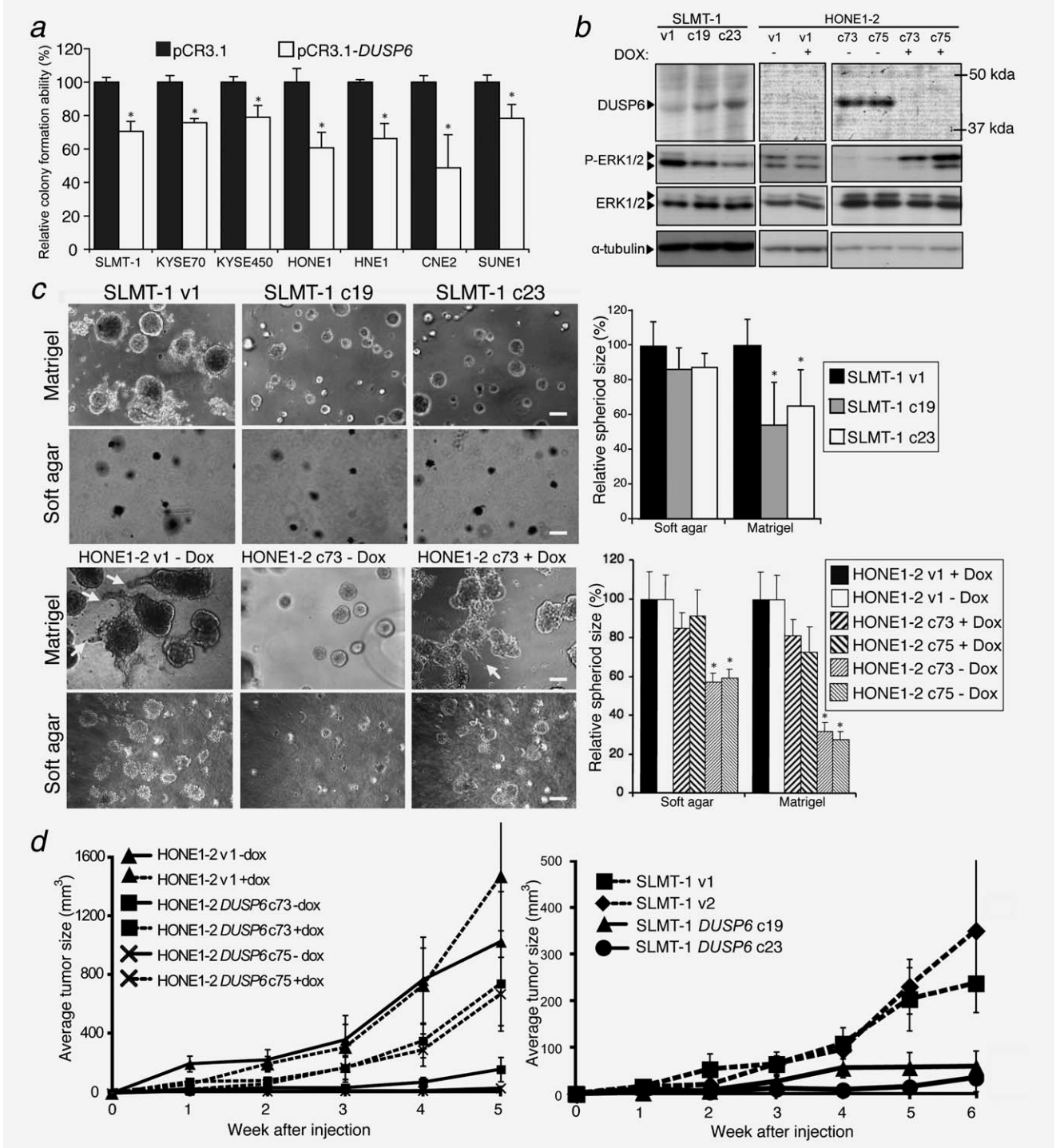

transcriptional start site, which overlapped with the CpG island (−1869 to −1379) predicted by Methprimer (http://www.urogene.org/methprimer/index1.html) (Fig. 2*b*). Bisulfite sequencing was used to analyze the 57 CpG sites in the CpG island. Higher methylation was observed in cancer cell lines and tumor biopsies compared to the corresponding immortalized cell lines and normal tissue counterparts. For example, in NPC, HONE1 and CNE2 have a 20.1- and 16.9-fold down-regulation of *DUSP6*, respectively, compared to NP460. A higher degree of methylation, ranging from 30 to 100% in NPC cell lines versus 0–50% in immortalized cell lines, was observed (Fig. 2*c*). This suggested that higher methylation at the −1869 to −1379 region is associated with silencing *DUSP6* expression. E-26 transcription factors (ETS), ETS1 and ETS2, are known

downstream targets of ERK1/2 signaling.[31] They regulate *DUSP6* expression, conferring a negative feedback in oncogenic ERK signaling.[32] There are four ETS1 binding sites in the analyzed region, as predicted by MATCH (http://www.gene-regulation.com) (Figs. 2*b* and 2*c*). Higher methylation of the predicted ETS-1 binding sites was also observed in tumor tissues and ESCC and NPC cell lines compared to normal tissue counterparts and the immortalized cell lines, suggesting the methylation of these ETS1 binding sites may block *DUSP6* transcription, leading to loss of a negative feedback control of the ERK activation. Of note, methylation-specific PCR was performed for the intron 1 region of *DUSP6*, in which hypermethylation is correlated with lower *DUSP6* expression in pancreatic cancer.[10] However, no correlation of methylation status and expression of *DUSP6* could be found, when comparing immortalized and cancer cell lines in ESCC and NPC (data not shown). This is reminiscent of the study done by Okudela et al.[9] in lung cancer, in which no correlation between methylation at intron 1 and *DUSP6* expression was found; the reason for this may possibly be attributed to differences in cancers analyzed.

Allelic loss in ESCC and NPC paired biopsies was analyzed by microsatellite analysis of the chromosome 12q21 region. Five microsatellite markers (D12S1719, D12S82, D12S1567, D12S1064 and D12S351) were used, mapping from 87.16 to 91.90 Mb around the *DUSP6* locus on 12q21 region. Loss was observed in 12q21 region, especially for the D9S1567 marker, which maps to the *DUSP6* region (Fig. 2*d* left). Representative microsatellite analysis shows allelic loss directly in tumor tissues (Fig. 2*d* right). Thus, the frequent loss of *DUSP6* expression in ESCC and NPC we found is consistent with both epigenetic silencing and allelic loss.

Assessment of the tumor suppressive ability of DUSP6 *in vitro* and *in vivo*

To assess the role of DUSP6 in cancer cell proliferation, three ESCC cell lines (SLMT-1, KYSE70 and KYE450) and four NPC cell lines (HONE1, HNE1, CNE2 and SUNE1) were examined by colony formation assay. Significant suppression of colony formation ability was observed in *DUSP6* transient transfectants compared to vector-alone controls (Fig. 3*a*). We stably expressed *DUSP6* in SLMT-1 and HONE-1 cell lines, which are highly tumorigenic and have down-regulated expression of DUSP6. In the NPC cell lines, we used a tetracycline-responsive vector for HONE1-2. Tetracycline treatment inactivates the tTA transcriptional activator, resulting in reduction of the ectopic expression of the transgene. The ectopic expression of *DUSP6* in HONE1-2 c73 and c75 dropped to levels similar to that of vector-alone after Dox treatment. Next, since DUSP6 is well-described to selectively inhibit activity of ERK by dephosphorylating the threonine and tyrosine residues,[4] we examined whether DUSP6 affects ERK activity by detecting the levels of phospho-ERK and ERK expression in the *DUSP6* stable clones. Ectopically expressed *DUSP6* significantly reduced the level of phospho-ERK, but not ERK, in *DUSP6* stably expressing clones [SLMT-1 c19 and c23; HONE1-2 c73 and c75 (-Dox)] (Fig. 3*b*), demonstrating the functional impact of DUSP6 in inhibiting the MARK signaling cascade in NPC and ESCC.

The functional impact of DUSP6 in tumorigenesis-associated properties was examined by anchorage-independent culture, three-dimensional reconstituted basement membrane (Matrigel) culture and *in vivo* tumorigenicity assays. In HONE1-2, overexpression of *DUSP6* confers tumor suppressive effects, with significantly smaller sized spheroids in soft

Figure 3. Assessment of the tumor suppressive ability of *DUSP6* in *in vitro* and *in vivo* functional studies. (*a*) Colony formation assay of three ESCC cell lines (SLMT-1, KYSE70 and KYSE450) and four NPC cell lines (HONE1, HNE1, CNE2 and SUNE1). After transient transfection with pCR3.1-*DUSP6*, significant suppression of colony formation was observed relative to vector-alone. * $p < 0.05$, compared to the corresponding pCR3.1 vector-alone transfected cell line. (*b*) Generation of stable *DUSP6* overexpressing clones in the SLMT-1 ESCC cell line and the HONE1-2 NPC cell line. SLMT-1 v1 and HONE1-2 v1 are vector-alone transfectants. SLMT-1 c19 and c23 and the HONE1-2 c73 and c75 are *DUSP6* overexpressing clones. In HONE1-2 c73 and c75, *DUSP6* overexpression is reduced in the presence of doxycycline. The specific substrate of DUSP6, ERK1/2, was dephosphorylated, when DUSP6 was overexpressed. α-tubulin serves as an equal loading control. (*c*) Soft agar and Matrigel culture. Upper panel: In Matrigel but not soft agar cultures, for SLMT-1 clones significantly smaller-sized spheroids were observed in *DUSP6* overexpressing clones (SLMT-1 c19 and c23) compared to the vector-alone stable clone (SLMT-1 v1). Lower panel: In both soft agar and Matrigel cultures, with HONE1-2 clones, significantly smaller-sized spheroids were observed in *DUSP6* overexpressing clones (HONE1-2 c73 and c75) compared to vector-alone stable clone (HONE1-2 v1). *$p < 0.05$, compared to the vector-alone control and their corresponding plus doxycycline control. Morphologically, in both SLMT-1 and HONE1-2, *DUSP6* overexpressing clones form well-organized and polarized spheroids compared to vector-alone clones. Protrusive structures from the spheroids (arrow) are observed in vector-alone (HONE1-2 v1) and in the *DUSP6* overexpressing clones (HONE1-2 c73 and c75) treated with doxycycline. However, these are not observed when *DUSP6* is overexpressed in the absence of doxycycline. Representative images are shown. (*d*) *In vivo* tumorigenicity assay of *DUSP6* stable clones and vector-alone controls (± doxycycline). In both SLMT-1 and HONE1-2 clones, significant suppression of tumor formation was observed in *DUSP6* overexpressing clones compared to vector-alone stable clones and *DUSP6* clones (+ doxycycline) 5–6 weeks after injection. Tumor sizes and statistical analysis are shown in Supplementary Table 2.

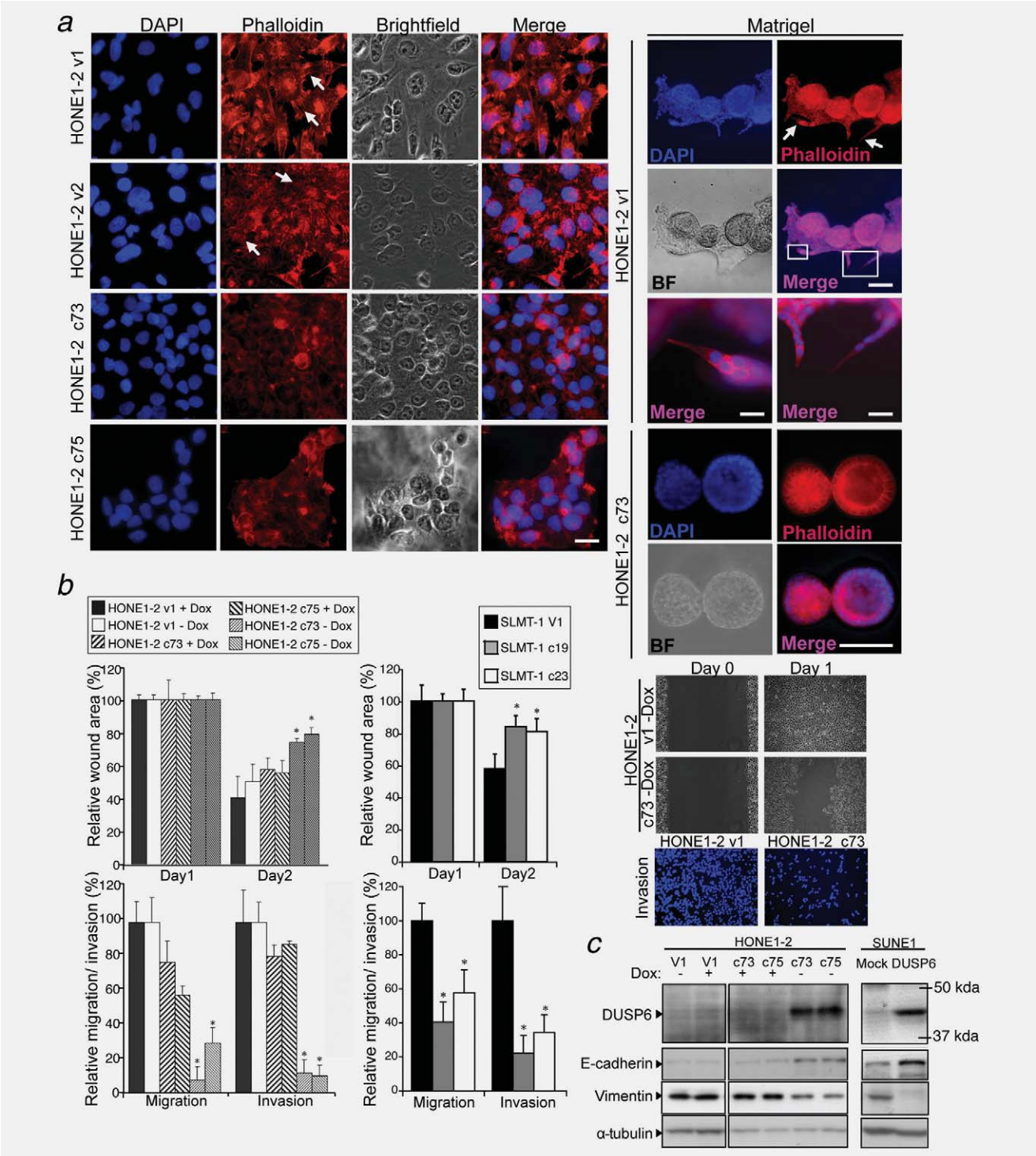

agar assay and Matrigel culture and reduced tumorigenicity in nude mouse assays being observed in *DUSP6* stable clones compared to vector-alone controls (Fig. 3*c*). In SLMT-1, *DUSP6*-expressing clones also show reduced size of spheroids for Matrigel culture and tumors in nude mouse assays compared to vector-alone controls, respectively (Fig. 3*d*). However, no perceptible difference was observed in the soft agar assay comparing SLMT-1 *DUSP6* overexpressing clones and the vector-alone clone, suggesting the tumor suppressive effect of DUSP6 in this cell line may require signaling stimulus from the tumor microenvironment. A more physiologically relevant condition is recapitulated in Matrigel culture and in *in vivo* nude mouse conditions. Notably, morphologically, in both SLMT-1 and HONE1-2 cell lines, *DUSP6*

overexpressing clones form well-organized and polarized spheroids compared to vector-alone clones. Protrusive structures from the spheroids are observed in vector-alone (HONE1-2 v1) and in the *DUSP6* overexpressing clones (HONE1-2 c73 and c75) treated with Dox. However, these are not observed when *DUSP6* is overexpressed in the absence of Dox (Fig. 3*c*). In *in vivo* tumorigenicity assays, significant suppression of tumor size was observed in the *DUSP6* overexpressing clones [SLMT-1 c19 and c23; HONE1-2 c73 and c75 (-Dox)], as compared to corresponding vector-alone clones [SLMT-1 v1; HONE1-2 v1 (-Dox)] (Fig. 3*d* and Supplementary Table 2). SLMT-1 v1 and v2 show a latency period of 4 weeks; HONE1-2 v1 and v2 and *DUSP6* overexpressing clones (HONE1-2 c73 and c75) treated with Dox show a latency period of 1–2 weeks. Strikingly, tumor size did not even reach 100 mm^3 by week 7 after injection in the *DUSP6* overexpressing clones [SLMT-1 c19 and c23; HONE1-2 c75 (-Dox)]. When the ectopic expression of DUSP6 was suppressed after Dox treatment, the suppression of tumor formation by DUSP6 was significantly reduced. The tumor suppressive effect of DUSP6 in ESCC and NPC was clearly evident *in vitro* and *in vivo*.

DUSP6 is involved in EMT-associated properties

During EMT, the cells become less adhesive to neighboring cells and basement membranes, leading to loss of the apical-basal polarity. In Matrigel culture, vector-alone stable clones (HONE1-1 v1) and *DUSP6* overexpressing clones treated with Dox (HONE1-2 c73 and c75) show a disorganized noncohesive and irregular morphology with protrusions, while in contrast, *DUSP6* overexpressing clones without Dox treatment (HONE1-2 c73 and c75) show polarized and well-organized spheroids (Figs. 3*b* and 4*a*). This morphological difference may be attributed to EMT-associated properties.[33] During EMT, epithelial cancer cells transform to a mesenchymal-like state, acquiring a high migratory ability to facilitate tumor metastasis. Metastatic cancer cells reduce their cell–cell adhesion and modify their actin cytoskeleton to migrate. The definition of mesenchymal cell is based on morphology and invasiveness; they have the properties of elongated morphology, extending filopodia and invasive motility.[34] We determined whether DUSP6 plays a role in EMT by evaluating several EMT-associated properties including actin skeleton alteration (formation of filopodia and lamellipodia), behavioral change (cell invasiveness) and expression of EMT markers (E-cadherin and vimentin). The clones grown on two- and three-dimensional culture were stained with phalloidin to investigate the actin cytoskeleton. In Matrigel culture, morphologically, vector-alone stable clones (HONE1-1 v1) and *DUSP6* overexpressing clones treated with Dox (HONE1-2 c73 and c75) displayed a pattern of elongated leading and trailing cells migrating out from the protrusive portion, resembling the mesenchymal phenotype.[34] Filopodia and lamellipodia are distinct actin-rich protrusions at the leading edge of motile cells essential for cell migration and invasion.[35] Extensive formation of filopodia and lamellipodia was obvious in vector-alone stable clones, while a regular pattern of cortical actin cytoskeleton detected between cell–cell boundaries was observed in *DUSP6* overexpressing clones (HONE1-2 c73 and c75) (Fig. 4*a*). These distinct morphologies suggest a potential impact of *DUSP6* in suppressing protrusiveness and EMT-associated phenotypes.

An essential functional consequence of EMT is the gain of cell migration and invasion abilities. Therefore, we used wound healing, cell migration chamber and cell invasion chamber assays to assess suppressive effects of DUSP6. Significant inhibition of wound healing ability, cell migration and invasion were observed in *DUSP6* overexpressing clones [SLMT-1 c19 and c23; HONE1-2 c73 and c75 (-Dox)], as compared to vector-alone stable clones (SLMT-1; HONE1-1 v1) and corresponding Dox-treated control (Fig. 4*b*). These findings confirm the potential impact of DUSP6 expression on tumor suppression. In addition to morphological and cell biological changes, EMT-associated change of gene expression

Figure 4. Investigating the cell migration and invasion suppressive abilities of *DUSP6*. (*a*) Staining of actin filaments by rhodamine phalloidin. Left panel: In two-dimensional culture, abundant filapodia and lamellipodial-like protrusions (indicated by arrow) were observed in two vector-alone stable clones (HONE1-2 v1 and v2) compared to *DUSP6* overexpressing clones (HONE1-2 c73 and c75). Scale bar: 100 μm. Right panel: In the spheroids grown in three-dimensional Matrigel culture, *DUSP6* overexpressing clones (HONE1-2 c73 and c75) form polarized cell spheroids, while the vector-alone clone (HONE1-2 v1) show a disorganized noncohesive morphology with protrusions (indicated by arrow): the protrusive structures are shown under higher magnification. DAPI: DNA stain. BF: brightfield. Scale bar: 100 μm; for magnified images, scale bar: 20 μm. Representative images are shown. When comparing SLMT-1 vector-alone and *DUSP6* overexpressing stable clones, no obvious differences in actin filament staining were observed (data not shown). (*b*) In wound healing, migration and invasion chamber assays, significant suppression of cell motility was observed in *DUSP6* overexpressing clones compared to vector-alone clones and their corresponding plus doxycycline control. Captured images are shown at 200*x* magnification. Bar charts of the relative wound area in wound healing assay and relative migration and invasion abilities are shown at the left. Representative images are shown at the right. **p*-value $<$ 0.05, compared to vector-alone and corresponding plus doxycycline control. (*c*) Alteration of the expression of EMT-associated markers by *DUSP6* overexpression. Left panel: When *DUSP6* was overexpressed in HONE1-2 c73 and HONE1-2 c75, increased expression of E-cadherin and decreased expression of vimentin are observed compared to vector-alone stable clones (HONE1-2 v1) and corresponding plus doxycycline control. Right panel: When *DUSP6* was transiently transfected in SUNE1, increased expression of E-cadherin and decreased expression of vimentin was observed. [Color figure can be viewed in the online issue, which is available at wileyonlinelibrary.com.]

has been well-described.[33] Thus, we investigated the change of well-characterized EMT markers such as epithelial marker E-cadherin[36] and mesenchymal marker vimentin.[37] Up-regulated E-cadherin and down-regulated vimentin were observed in *DUSP6* overexpressing clones [HONE1-2 c73 and c75 (-Dox)], as compared to vector-alone stable clones (HONE1-1 v1) and the corresponding +Dox control (Fig. 4*c*). The altered expression of E-cadherin and vimentin in *DUSP6* overexpressing clones (HONE1-2 c73 and c75) is restored after Dox treatment. Another NPC cell line, SUNE1, was transiently transfected with the *DUSP6* vector. The same pattern of change of EMT markers was observed in *DUSP6*-transient transfectants compared to the vector-alone control. Taken together, based on the EMT-associated events being evaluated, these data suggest a potential role of DUSP6 in suppressing invasiveness and EMT-associated properties.

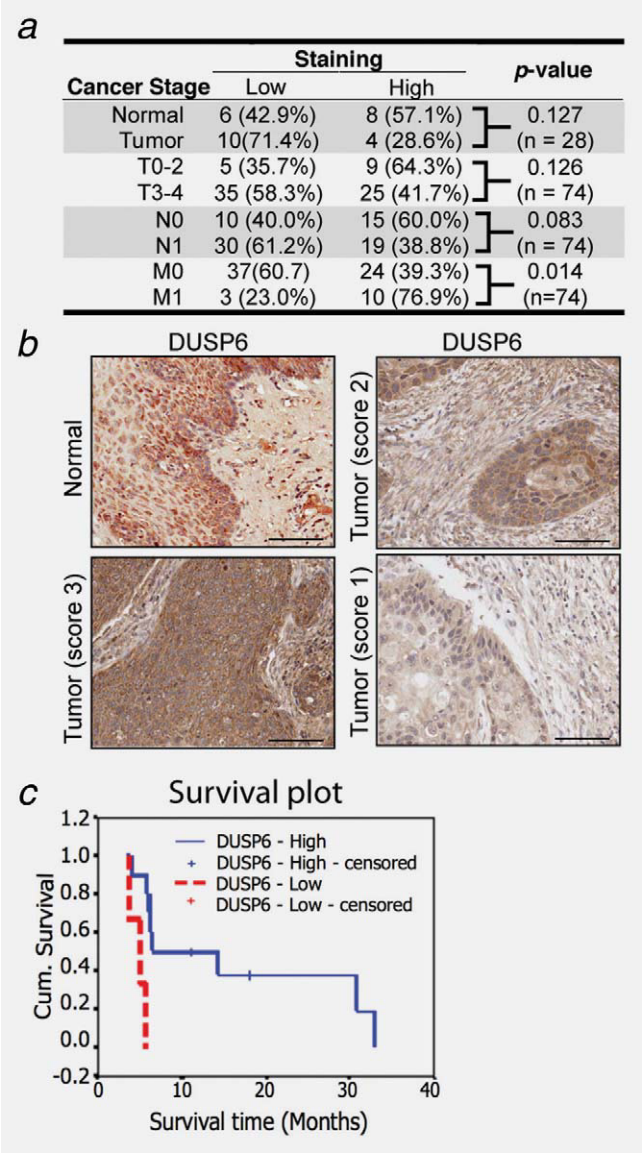

Figure 5. Evaluation of clinical significance of DUSP6 by tissue microarray (TMA) analysis. (*a*) Comparison of DUSP6 and clinical parameters. In the Hong Kong ESCC patient TMA, a trend of abrogation of DUSP6 expression was found in tumor tissues compared to matched normal, tumor tissues of stages T3-4 compared to T0-2, and of stages N1 compared to N0. Significantly increased DUSP6 expression was observed in tumor tissues of M1 compared to M0. (*b*) Representative images of immunohistochemical staining from TMA study. Normal = normal-appearing mucosa from an esophagectomy specimen. Among 74 tumor tissues in TMA study, six were scored as 0, 34 as 1, 25 as 2 and 9 as 3. Tumor tissues with scores 1, 2 and 3, representing weak, moderate, and strong staining of DUSP6, respectively, are illustrated (scale bar, 100 μm) (*c*) Survival curve of ESCC patients with presence of distant metastasis. In Kaplan–Meier statistical analysis, stage M1 patients with higher expression of DUSP6 have significantly improved survival compared to patients with lower DUSP6 expression, with mean survivals of 16.59 months (95% CI: 8.35 - 24.83) and 4.75 months (95% CI: 3.51 – 5.99), respectively ($n = 13$, $p = 0.0018$). [Color figure can be viewed in the online issue, which is available at wileyonlinelibrary.com.]

ESCC tissue microarray analysis shows DUSP6 expression is associated with tumor stage and survival of M1 patients

With an important role of DUSP6 in suppressing tumor growth and cancer dissemination, we would expect DUSP6 to affect the clinical outcome of ESCC treatment. Thus, TMA IHC staining was conducted using specimens from Hong Kong ESCC patients. The tissue types and tumor stages of 74 cases and 26 normal controls are shown in Supplementary Table 2. A trend of abrogated DUSP6 expression was found in: (*i*) tumor tissues compared to matched normal (chi-square test, $p = 0.127$, $n = 28$); (*ii*) tumor tissues of stages T3-4 compared to T0-2 (chi-square test, $p = 0.126$, $n = 74$); and (*iii*) tumor tissues of stages N1 compared to N0 (chi-square test, $p = 0.083$, $n = 74$) (Fig. 5*a*). Interestingly, significant up-regulated DUSP6 expression was observed in tumor tissues of stage M1 compared to M0 (chi-square test, $p = 0.014$, $n = 74$). Significantly and more importantly, by Kaplan–Meier statistical analysis, in patients diagnosed with distant metastasis (M1 stage), higher DUSP6 expression in tumor specimens was observed to correlate with longer patient survival compared to patients with lower DUSP6 expression, with a mean survival of 16.59 months (95% CI: 8.35−24.83), compared to 4.75 months (95% CI: 3.51–5.99), respectively ($n = 13$, $p = 0.0018$) (Fig. 5*c*). The observed up-regulation of DUSP6 expression in patients diagnosed with distant metastasis (M1 stage) may be a result of a negative feedback loop in response to oncogenic signaling of cancer cells during metastatic progression.

Discussion

DUSP6 appears to play an important role in ESCC and NPC. Our results demonstrate that DUSP6 is (*i*) frequently down-

regulated in cancer cell lines and tumor tissues by quantitative PCR and Western blotting; (*ii*) tumor suppressive by colony formation, soft agar and Matrigel culture and *in vivo* tumorigenicity assays; and (*iii*) cell migration- and invasion-suppressive by wound healing, cell migration and cell invasion chamber assays. Furthermore, a potential involvement of DUSP6 in suppressing EMT-associated properties was observed by examining the morphology of cell spheroids in three-dimensional culture, formation of filopodia and lamellipodia, cell migration and invasion abilities and expression of EMT markers such as E-cadherin and vimentin.

Gene and protein expression analyses identified frequent loss of DUSP6 in ESCC and NPC cell lines and tumor biopsies, suggesting a pivotal role of DUSP6 in tumor development. In line with these results, ESCC TMA analysis revealed an association of DUSP6 expression with better patient survival, further supporting the key role of DUSP6 in tumor development and metastasis. Mechanisms for DUSP6 gene down-regulation were investigated. BGS analysis of the CpG island located at the predicted promoter region of *DUSP6* and the demethylation treatment of cancer cell lines suggested epigenetic silencing may contribute to loss of DUSP6 in ESCC and NPC, although only a few tissue biopsies were examined due to limited amounts of available tissues. Allelic loss of 12q21, where *DUSP6* maps, was also found using ESCC and NPC tumor specimens and is consistent with earlier studies showing chromosome 12q is a commonly deleted region in ESCC and NPC.[17,18]

Our functional analyses demonstrate the tumor suppressive effect of DUSP6 in ESCC and NPC. DUSP6 selectively inactivates ERK1/2, providing a negative feedback loop in the MARK signaling pathway.[1] The MAPK family includes the ERKs and the Stress-Activated Protein kinases (SAPKs) p38 and JNK. ERK/ MAPK signaling is frequently activated and promotes cancer cell proliferation, cell survival and metastasis.[3,38] The activation of ERK1/2 promotes cancer cell proliferation in ESCC[22] and NPC.[23] Positive p-ERK expression was correlated with poorer survival and advanced clinical stage in NPC.[39] The reduced activity of ERK in DUSP6 overexpressing clones may contribute to the tumor suppressive effects of DUSP6. The underlying molecular mechanism for this warrants further investigation.

EMT not only plays a crucial role during developmental processes but also confers onto cancer cells a metastatic capability to disseminate to distant sites.[40] Indeed, studies in drosophila, zebrafish, xenopus and chick embryos have suggested that DUSP6 plays a crucial role in embryonic development.[41–43] DUSP6 was found to regulate cell adhesion.[44] Additionally, DUSP6 expression was down-regulated in invasive carcinomas.[6] Recent work of Shin et al.[24] showed the role of ERK2 in promoting cell invasion and EMT. DUSP6 is functionally and physically associated with ERK2 and selectively inhibits its activity.[1,45] These lines of evidence suggest a potential impact of DUSP6 in cancer cell motility and EMT, which has not yet been reported. This functional study examining the morphological, cell behavioral and EMT-associated gene expression alterations now provides evidence supporting this possibility. During the EMT, the apical-basal polarity and cell–cell adhesion of the cells were lost. Cell invasiveness and EMT-associated phenotypes such as the acinar structure were observed in cells grown in the Matrigel 3D culture conditions mimicking the tumor environment.[46] The polarized cell spheroid formation in *DUSP6*-expressing clones suggests a phenotypic reversion that displays epithelial polarity and provides pivotal clues for a role of DUSP6 in suppressing cell invasiveness and EMT-associated properties. More importantly, dramatic suppression of cell migration and invasion in *DUSP6* overexpressing clones further confirms the suppressive role of DUSP6. The expression of E-cadherin and vimentin are associated with survival and are independent prognostic indicators. The down-regulation of E-cadherin and up-regulation of vimentin are associated with tumor recurrence and death.[47] Loss of E-cadherin, a well-defined epithelial marker, disrupts intercellular contacts and induces EMT.[36] In NPC, loss of E-cadherin closely associates with advanced tumor stage and lymph node metastasis.[48] Increased expression of vimentin, a mesenchymal marker, promotes cell motility and EMT.[37] The observed change of EMT markers in *DUSP6* overexpressing clones of HONE1-2 further suggested an impact of DUSP6 in EMT. The detailed mechanism underlying this commitment requires further study. In SLMT-1, although impaired cell motility was observed in *DUSP6*-expressing clones, the alteration of EMT marker expression was not pronounced (data not shown). Of note, in SLMT-1, virtually no vimentin protein expression can be detected. The molecular event underlying these differences may be due to differences in tumor types and pathogenesis. Indeed, in ESCC, no vimentin expression in both primary and metastatic carcinomas has been reported.[49] In the absence of EMT, cancer cells can also use a broad repertoire of strategies to migrate.[50]

Expanding lines of evidence suggest an impact of oncogenic ERK mutation in tumorigenesis;[3,38] however, the role of its negative regulator, DUSP6, has not yet been characterized in ESCC and NPC. We now provide clear evidence supporting *DUSP6* as a critical gene capable of suppressing tumorigenesis and invasiveness. In NPC, DUSP6 suppresses EMT-associated phenotypes. Additionally, we demonstrate a clinical relevance of DUSP6 in cancers. Understanding regulation of the ERK pathway is of considerate interest in developing rational therapeutic strategies and to sensitize the tumor towards conventional therapy. Additional studies are needed to unravel the molecular mechanism of DUSP6, a negative regulator of ERK in tumorigenesis.

Acknowledgements

The authors thank DSMZ (German Collection of Microorganisms and Cell Culture) for KYSE cell lines.[26] The authors acknowledge the University Grants Council of Hong Kong Special Administrative Region, People's Republic of China (Area of Excellence grant AoE/M-06/08) and the University of Hong Kong Seed Funding Programme for Basic Research for funding support to M.L.L. and the Swedish Cancer Society, the Swedish Research Council, the Swedish Institute, and Karolinska Institute to E.R.Z.

References

1. Arkell RS, Dickinson RJ, Squires M, Hayat S, Keyse SM, Cook SJ. DUSP6/MKP-3 inactivates ERK1/2 but fails to bind and inactivate ERK5. *Cell Signal* 2008;20: 836–43.
2. Dhillon AS, Hagan S, Rath O, Kolch W. MAP kinase signalling pathways in cancer. *Oncogene* 2007;26:3279–90.
3. Hoshino R, Chatani Y, Yamori T, Tsuruo T, Oka H, Yoshida O, Shimada Y, Ari-i S, Wada H, Fujimoto J, Kohno M. Constitutive activation of the 41-/43-kDa mitogen-activated protein kinase signaling pathway in human tumors. *Oncogene* 1999; 18:813–22.
4. Patterson KI, Brummer T, O'Brien PM, Daly RJ. Dual-specificity phosphatases: critical regulators with diverse cellular targets. *Biochem J* 2009;418:475–89.
5. Jurek A, Amagasaki K, Gembarska A, Heldin CH, Lennartsson J. Negative and positive regulation of MAPK phosphatase 3 controls platelet-derived growth factor-induced Erk activation. *J Biol Chem* 2009; 284:4626–34.
6. Furukawa T, Sunamura M, Motoi F, Matsuno S, Horii A. Potential tumor suppressive pathway involving DUSP6/ MKP-3 in pancreatic cancer. *Am J Pathol* 2003;162:1807–15.
7. Furukawa T, Fujisaki R, Yoshida Y, Kanai N, Sunamura M, Abe T, Takeda K, Matsuno S, Horii A. Distinct progression pathways involving the dysfunction of DUSP6/MKP-3 in pancreatic intraepithelial neoplasia and intraductal papillary-mucinous neoplasms of the pancreas. *Mod Pathol* 2005;18:1034–42.
8. Chan D, Liu V, Tsao G, Yao K, Furukawa T, Chan K, Ngan H. Loss of MKP3 mediated by oxidative stress enhances tumorigenicity and chemoresistance of ovarian cancer cells. *Carcinogenesis* 2008; 29:1742–50.
9. Okudela K, Yazawa T, Woo T, Sakaeda M, Ishii J, Mitsui H, Shimoyamada H, Sato H, Tajiri M, Ogawa N, Masuda M, Takahashi T, et al. Down-regulation of DUSP6 expression in lung cancer: its mechanism and potential role in carcinogenesis. *Am J Pathol* 2009;175:867–81.
10. Xu S, Furukawa T, Kanai N, Sunamura M, Horii A. Abrogation of DUSP6 by hypermethylation in human pancreatic cancer. *J Hum Genet* 2005;50:159–67.
11. MacKeigan JP, Murphy LO, Blenis J. Sensitized RNAi screen of human kinases and phosphatases identifies new regulators of apoptosis and chemoresistance. *Nat Cell Biol* 2005;7:591–600.
12. Cui Y, Parra I, Zhang M, Hilsenbeck SG, Tsimelzon A, Furukawa T, Horii A, Zhang ZY, Nicholson RI, Fuqua SA. Elevated expression of mitogen-activated protein kinase phosphatase 3 in breast tumors: a mechanism of tamoxifen resistance. *Cancer Res* 2006;66:5950–9.
13. Lonne GK, Masoumi KC, Lennartsson J, Larsson C. Protein kinase Cdelta supports survival of MDA-MB-231 breast cancer cells by suppressing the ERK1/2 pathway. *J Biol Chem* 2009;284:33456–65.
14. Chiappinelli KB, Rimel BJ, Massad LS, Goodfellow PJ. Infrequent methylation of the DUSP6 phosphatase in endometrial cancer. *Gynecol Oncol* 2010;119:146–50.
15. Titcomb CP, Jr. High incidence of nasopharyngeal carcinoma in Asia. *J Insur Med* 2001;33:235–8.
16. Li JY. Epidemiology of esophageal cancer in China. *Natl Cancer Inst Monogr* 1982; 62:113–20.
17. Mayama T, Fukushige S, Shineha R, Nishihira T, Satomi S, Horii A. Frequent loss of copy number on the long arm of chromosome 21 in human esophageal squamous cell carcinoma. *Int J Oncol* 2000; 17:245–52.
18. Lo KW, Teo PM, Hui AB, To KF, Tsang YS, Chan SY, Mak KF, Lee JC, Huang DP. High resolution allelotype of microdissected primary nasopharyngeal carcinoma. *Cancer Res* 2000;60:3348–53.
19. Chen X, Ma WL, Liang S, Liao ZJ, Shang T, Zheng WL. [Effect of Epstein-Barr virus reactivation on gene expression profile of nasopharyngeal carcinoma]. *Ai Zheng* 2008;27:1–7.
20. Yang L, Leung AC, Ko JM, Lo PH, Tang JC, Srivastava G, Oshimura M, Stanbridge EJ, Daigo Y, Nakamura Y, Tang CM, Lau KW, et al. Tumor suppressive role of a 2.4 Mb 9q33-q34 critical region and DEC1 in esophageal squamous cell carcinoma. *Oncogene* 2005;24:697–705.
21. Leung AC, Wong VC, Yang LC, Chan PL, Daigo Y, Nakamura Y, Qi RZ, Miller LD, Liu ET, Wang LD, Li JL, Law S, et al. Frequent decreased expression of candidate tumor suppressor gene, DEC1, and its anchorage-independent growth properties and impact on global gene expression in esophageal carcinoma. *Int J Cancer* 2008; 122:587–94.
22. Liu X, Wu WK, Yu L, Sung JJ, Srivastava G, Zhang ST, Cho CH. Epinephrine stimulates esophageal squamous-cell carcinoma cell proliferation via beta-adrenoceptor-dependent transactivation of extracellular signal-regulated kinase/ cyclooxygenase-2 pathway. *J Cell Biochem* 2008;105:53–60.
23. Wu M, Li X, Li G. Signaling transduction network mediated by tumor suppressor/ susceptibility genes in NPC. *Curr Genomics* 2009;10:216–22.
24. Shin S, Dimitri CA, Yoon SO, Dowdle W, Blenis J. ERK2 but not ERK1 induces epithelial-to-mesenchymal transformation via DEF motif-dependent signaling events. *Mol Cell* 2010;38:114–27.
25. Wong VC, Chan PL, Bernabeu C, Law S, Wang LD, Li JL, Tsao SW, Srivastava G, Lung ML. Identification of an invasion and tumor-suppressing gene, Endoglin (ENG), silenced by both epigenetic inactivation and allelic loss in esophageal squamous cell carcinoma. *Int J Cancer* 2008;123:2816–23.
26. Shimada Y, Imamura M, Wagata T, Yamaguchi N, Tobe T. Characterization of 21 newly established esophageal cancer cell lines. *Cancer* 1992;69:277–84.
27. Li HM, Man C, Jin Y, Deng W, Yip YL, Feng HC, Cheung YC, Lo KW, Meltzer PS, Wu ZG, Kwong YL, Yuen AP, et al. Molecular and cytogenetic changes involved in the immortalization of nasopharyngeal epithelial cells by telomerase. *Int J Cancer* 2006;119:1567–76.
28. Protopopov AI, Li J, Winberg G, Gizatullin RZ, Kashuba VI, Klein G, Zabarovsky ER. Human cell lines engineered for tetracycline-regulated expression of tumor suppressor candidate genes from a frequently affected chromosomal region, 3p21. *J Gene Med* 2002;4:397–406.
29. Lung HL, Bangarusamy DK, Xie D, Cheung AK, Cheng Y, Kumaran MK, Miller L, Liu ET, Guan XY, Sham JS, Fang Y, Li L, et al. THY1 is a candidate tumour suppressor gene with decreased expression in metastatic nasopharyngeal carcinoma. *Oncogene* 2005;24:6525–32.
30. Yuen HF, Chan YP, Chan KK, Chu YY, Wong ML, Law SY, Srivastava G, Wong YC, Wang X, Chan KW. Id-1 and Id-2 are markers for metastasis and prognosis in oesophageal squamous cell carcinoma. *Br J Cancer* 2007;97:1409–15.
31. Yang SH, Sharrocks AD, Whitmarsh AJ. Transcriptional regulation by the MAP kinase signaling cascades. *Gene* 2003;320: 3–21.
32. Zhang Z, Kobayashi S, Borczuk AC, Leidner RS, Laframboise T, Levine AD, Halmos B. Dual specificity phosphatase 6 (DUSP6) is an ETS-regulated negative feedback mediator of oncogenic ERK-signaling in lung cancer cells. *Carcinogenesis* 2010;31:577–86.
33. Huber MA, Kraut N, Beug H. Molecular requirements for epithelial-mesenchymal transition during tumor progression. *Curr Opin Cell Biol* 2005;17:548–58.
34. Hay ED. The mesenchymal cell, its role in the embryo, and the remarkable signaling

mechanisms that create it. *Dev Dyn* 2005; 233:706–20.
35. Mattila PK, Lappalainen P. Filopodia: molecular architecture and cellular functions. *Nat Rev Mol Cell Biol* 2008;9: 446–54.
36. Onder TT, Gupta PB, Mani SA, Yang J, Lander ES, Weinberg RA. Loss of E-cadherin promotes metastasis via multiple downstream transcriptional pathways. *Cancer Res* 2008;68: 3645–54.
37. Mendez MG, Kojima S, Goldman RD. Vimentin induces changes in cell shape, motility, and adhesion during the epithelial to mesenchymal transition. *FASEB J* 2010; 24:1838–51.
38. Roberts PJ, Der CJ. Targeting the Raf-MEK-ERK mitogen-activated protein kinase cascade for the treatment of cancer. *Oncogene* 2007;26:3291–310.
39. Wang SS, Guan ZZ, Xiang YQ, Wang B, Lin TY, Jiang WQ, Zhang L, Zhang HZ, Hou JH. [Significance of EGFR and p-ERK expression in nasopharyngeal carcinoma]. *Zhonghua Zhong Liu Za Zhi* 2006;28: 28–31.
40. Thiery JP, Acloque H, Huang RY, Nieto MA. Epithelial-mesenchymal transitions in development and disease. *Cell* 2009;139: 871–90.
41. Kawakami Y, Rodriguez-Leon J, Koth CM, Buscher D, Itoh T, Raya A, Ng JK, Esteban CR, Takahashi S, Henrique D, Schwarz MF, Asahara H, et al. MKP3 mediates the cellular response to FGF8 signalling in the vertebrate limb. *Nat Cell Biol* 2003;5:513–9.
42. Tsang M, Maegawa S, Kiang A, Habas R, Weinberg E, Dawid IB. A role for MKP3 in axial patterning of the zebrafish embryo. *Development* 2004;131:2769–79.
43. Gomez AR, Lopez-Varea A, Molnar C, de la Calle-Mustienes E, Ruiz-Gomez M, Gomez-Skarmeta JL, de Celis JF. Conserved cross-interactions in Drosophila and Xenopus between Ras/MAPK signaling and the dual-specificity phosphatase MKP3. *Dev Dyn* 2005;232:695–708.
44. Glading A, Uberall F, Keyse SM, Lauffenburger DA, Wells A. Membrane proximal ERK signaling is required for M-calpain activation downstream of epidermal growth factor receptor signaling. *J Biol Chem* 2001;276:23341–8.
45. Camps M, Nichols A, Gillieron C, Antonsson B, Muda M, Chabert C, Boschert U, Arkinstall S. Catalytic activation of the phosphatase MKP-3 by ERK2 mitogen-activated protein kinase. *Science* 1998;280:1262–5.
46. Shaw KR, Wrobel CN, Brugge JS. Use of three-dimensional basement membrane cultures to model oncogene-induced changes in mammary epithelial morphogenesis. *J Mammary Gland Biol Neoplasia* 2004;9:297–310.
47. Liu LK, Jiang XY, Zhou XX, Wang DM, Song XL, Jiang HB. Upregulation of vimentin and aberrant expression of E-cadherin/beta-catenin complex in oral squamous cell carcinomas: correlation with the clinicopathological features and patient outcome. *Mod Pathol* 2010;23: 213–24.
48. Zheng Z, Pan J, Chu B, Wong YC, Cheung AL, Tsao SW. Downregulation and abnormal expression of E-cadherin and beta-catenin in nasopharyngeal carcinoma: close association with advanced disease stage and lymph node metastasis. *Hum Pathol* 1999; 30:458–66.
49. Jin H, Morohashi S, Sato F, Kudo Y, Akasaka H, Tsutsumi S, Ogasawara H, Miyamoto K, Wajima N, Kawasaki H, Hakamada K, Kijima H. Vimentin expression of esophageal squamous cell carcinoma and its aggressive potential for lymph node metastasis. *Biomed Res* 2010; 31:105–12.
50. Friedl P. Prespecification and plasticity: shifting mechanisms of cell migration. *Curr Opin Cell Biol* 2004;16:14–23.